Volume 1 | Number 1 | Jan 2013 | Pages 1–100

Journal of
Materials Chemistry C

Materials for optical and electronic devices
www.rsc.org/materialsC

ROYAL SOCIETY
OF CHEMISTRY

ROYAL SOCIETY
OF CHEMISTRY

www.rsc.org/materialsC

Journal Name

Journal of Materials Chemistry C

Dynamic Article Links ▶

ARTICLE TYPE

Highly Efficient Deep-Blue OLED with an Extraordinary Narrow FHWM of 35 nm and Y Coordinate < 0.05 Based on a Fully Twisting Donor-Acceptor Molecule

Weijun Li,[a] Liang Yao,[a] Haichao Liu,[a] Zhiming Wang,[a] Shitong Zhang,[a] Ran Xiao,[a] Huanhuan Zhang,[a]
5 **Ping Lu,[a] Bing Yang,[*a,b] and Yuguang Ma[a,c]**

A highly efficient deep-blue OLED based on a fully twisting donor-acceptor molecule TPA-PIM exhibited a maximum
10 **quantum efficiency of 3 % and a particular narrow electroluminescence emission peaked at 420 nm with a FHWM of only 35 nm and a CIE coordinate of (0.161, 0.046).**

Organic light-emitting diodes (OLEDs)[1] have attracted sustaining attention due to the potential use in flat displays
15 and lighting sources in the past decades. To date, numerous RGB (red, green and blue) molecular materials have been designed and synthesized to fabricate full color OLED displays.[2] However, the highly efficient deep blue emitter, which is quite important and absolutely necessary for the
20 white OLEDs as one of three basic colors and simultaneously the host for both green and red emitter in doped devices, is still a challenge, due to its intrinsic wide band gap and poor carrier balance from mismatched electronic energy level in device.[3] In the meantime, for an excellent deep blue emitter,
25 good color purity and CIE coordinate are also key factors in the OLED performance for the demand of color saturation in full-color display and lighting.[4] A perfect deep blue color requires a CIE coordinate of (0.15, 0.06) from the standard of European Broadcasting Union (EBU) as well as an excellent
30 color purity with both narrow full peak width and FWHM (full width at half maximum). The current deep blue emitters mainly based on the chromophore of fluorine,[5] and anthracene[6] have rarely met these requirements, though some of the electroluminescence (EL) efficiencies have reached the
35 very high level, mostly due to their wide emission range with a large FWHM or full peak width in the EL spectra. Now it is not a problem for the recently emerged phenanthro[9,10-*d*]imidazole[7] deriatives which may simultaneously show the high EL efficiencies, good CIE coordinates and narrow
40 FWHMs in EL spectra, indicating the phenanthro[9,10-*d*]imidazole should serve as the perfect building unit for designing the excellent deep-blue emitters.[8] Analysis of the electron transition configuration in phenanthro[9,10-*d*]imidazole deriatives indicates that, though the
45 phenanthro[9,10-*d*]imidazole structure behaves as a large rigid plane, the five-member imidazole ring mainly determines its electron transition[7,8] while the phenanthrene and vertically

substituted side phenyl ring contributes substantively little to the eletron transition.

50 Here, based on the five-member imidazole ring, we report a deep blue emissive fully twisting donor-acceptor molecule, N,N-diphenyl-4'-(1,4,5-triphenyl-1H-imidazol-2-yl)-[1,1'-biphenyl]-4-amine (TPA-PIM), which can be seen as a derivative from the previously reported excellent deep blue
55 emitter N,N-diphenyl-4'-(1-phenyl-1H-phenanthro[9,10-*d*]imidazol-2-yl)biphenyl-4-amine (TPA-PPI)[9] by breaking only a chemical bond in the phenanthrene part of phenanthro-[9,10-*d*]imidazole, as shown in Figure 1. Surprisingly, an extraordinary narrow EL emission with a FWHM of only 35
60 nm and CIE coordinate (0.161, 0.046) was observed in the OLED of TPA-PIM as the emitter, whose y value is the smallest ever reported. Simultaneously, TPA-PIM's device also exhibited a high quantum efficiency of 3%.
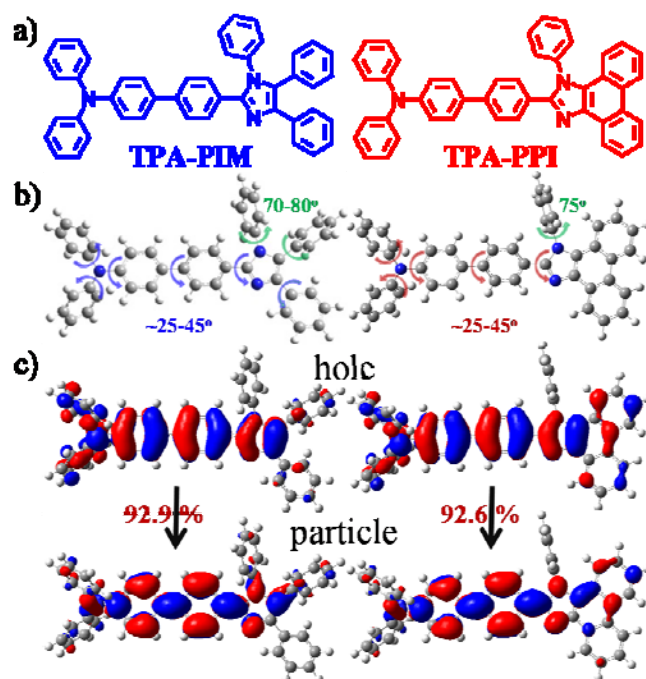

65 Figure 1. a) Molecular structure, b) optimized geometry with twist angles and c) natural transition orbital by DFT for two twisting donor-acceptor molecules TPA-PIM and TPA-PPI

TPA-PIM was synthesized by a Suzuki coupling reaction between borate triphenylamine and bromo-imidazole, which was obtained by a one-step cycling reaction, as shown in Figure S1. From the molecular structure, due to the break of the single bond in phenanthrene part, TPA-PIM totally becomes a combination of five-member imidazole and six-member phenyl rings, in the absence of the large rigid phenanthro[9,10-*d*]imidazole structure in TPA-PPI (Figure 1a). From the optimized geometry by density functional theory (DFT/B3LYP/6-31g**), the substituent phenyls are nearly perpendicular to the planar imidazole ring with large twist angles of 70~80 degree in TPA-PIM (Figure 1b), due to the large steric hindrance between adjacent substituent phenyl rings and the strong repulsion between neighboring hydrogen atoms. As a comparison, TPA-PIM shows a fully twisting structure, while TPA-PPI exhibits a partial twisting molecular structure with a large rigid phenanthro[9,10-*d*]imidazole plane.

To describe the emission nature, the lowest excited-states were optimized using time-dependent DFT calculations. The natural transition orbitals (NTO) demonstrated that TPA-PIM and TPA-PPI had the nearly same hole and particle wavefunction distributions as we predicted, in spite of the existence of a large rigid phenanthro[9,10-*d*]imidazole plane in TPA-PPI. As shown in Figure 1c, both hole and particle are mainly delocalized over the molecular backbone composed of five-member imidazole ring, middle phenyl bridge and triphenylamine for both TPA-PIM and TPA-PPI. The similar excited-state property indicates the similar photophysical properties between TPA-PIM and TPA-PPI. PL measurements showed that TPA-PIM displayed the nearly similar PL spectra characters with λ_{max} at 424 nm to that of TPA-PPI with λ_{max} at 438 nm (in Figure S2). A similar trend was also observed in their UV spectra. The solvatochromic experiments in different polar solvents also exhibited the similar behaviors between TPA-PIM and TPA-PPI, which presented the same nonlinear relationship between maximum wavenumber and solvent polarity, as well as the close excited-state dipole moments (Figure S3 and S4). This reminded a fact that an intercrossed LE and CT excited-state character also existed in TPA-PIM in the case of the moderate polarity solvent. The electrochemistry measurement showed the highest occupied molecular orbital (HOMO) level of -5.26 eV and the lowest unoccupied molecular orbital (LUMO) of -2.19 eV in TPA-PIM, which are close to those values[9] of TPA-PPI (Figure S5). The similar electronic energy levels also can be deduced from the photophysical spectra measurements. All of these data indicate that the only one single bond difference in molecular structure between TPA-PIM and TPA-PPI can hardly cause any change between their molecular properties.

Using quinine sulphate in 1 M sulphuric acid as a standard, we obtained a fluorescence quantum yield value as high as 75% for TPA-PIM in chloroform, simutaneously as well as a value of 60% in film by using an integrating-sphere photometer. Compared to the high efficiency 90% of TPA-PPI in both solution and film[9], TPA-PIM showed a relatively lower efficiency. For the reasons, the intramolecular vibration relaxtion is enhanced in the excited state of TPA-PIM due to a flexible fully twisting molecular structure in contrast with TPA-PPI with the larger rigidity, which effectively quenches the radiative excitons and induces the lower photoluminescence efficiency. Meantime, the more flexible molecular structure also caused the relatively worse thermal properties in TPA-PIM, exactly, a T_g of ~100 °C and a T_d of 375 °C at the weight percent of 95%, which are lower than those of TPA-PPI (Figure S6).
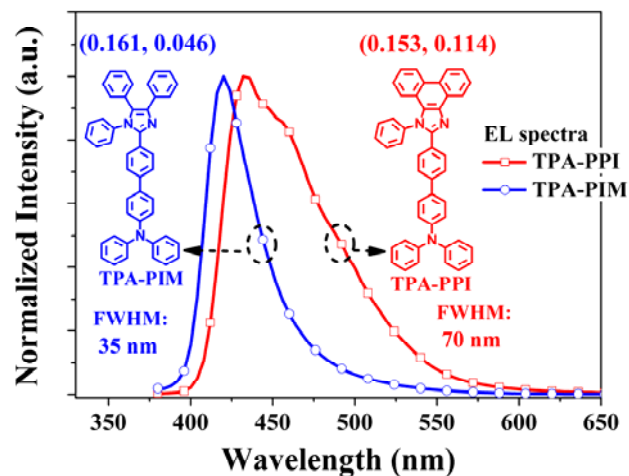

Figure 2. The electroluminescence spectra of TPA-PPI and TPA-PIM with their molecular structures, FWHM and 1931 CIE coordinate inset.

Although the tiny difference between TPA-PIM and TPA-PPI is one single bond in the molecular structure, this single bond produced a huge difference in their OLED performance, especially for the EL spectra or CIE coordinate. The OLEDs were fabricated with the frequently used multilayered structure: ITO/MoO$_3$ (10 nm) or PEDOT:PSS (40 nm)/ N,N′-di-1-naphthyl- N,N'-diphenylbenzidine (NPB) (80 nm)/ 4,4′,4″-tri(N-carbazolyl)-triphenylamine (TCTA) (5 nm)/TPA-PPI or TPA-PIM (20 nm)/ 1,3,5-tri(phenyl-2-benzimidazolyl)-benzene (TPBi) (40 nm)/LiF (1 nm)/Al (100 nm), in which MoO$_3$ and PEDOT:PSS were both utilized as a hole-injecting layer, NPB and TCTA as hole-transporting and buffer layers, and TPBi as an electron-transporting and hole-blocking layer. As shown in Figure 2, device based on TPA-PPI as emitter exhibited a highly efficient deep-blue EL with λ_{max} at 434 nm together with a CIE coordinate of (0.153, 0.114). Compared to TPA-PPI, TPA-PIM also showed a deep-blue EL emission with λ_{max} at 420 nm, but it exhibited a saturated and much deeper CIE coordinate of (0.161, 0.046), whose y value is even smaller in comparison to the EBU standard of (0.15. 0.06). A much smaller FWHM of 35 nm was observed in EL spectrum of TPA-PIM, which is half of the TPA-PPI (70 nm) (Figure 2). Thus the CIE coordinate difference between TPA-PIM and TPA-PPI should be mainly ascribed to the FWHM of their EL spectra, instead of the maximum EL peaks difference of less than 15 nm. As we known, 35 nm of FWHM was the narrowest value ever reported while 70 nm of FWHM was relatively normal.[8] By comparing the EL and PL spectra both under 77K and at room temperature (Figure S7), we found that the FWHM became gradually narrower from PL spectra at room temperature (56 nm) to 77K (48 nm), and to EL spectra (35 nm) in TPA-PIM case. Whereas in TPA-PPI case,

the FWHM of EL spectra (70 nm) was obviously larger than those of PL spectra at room temperature (60 nm) and under 77K (54 nm). An easy direct explanation for the narrowed EL than PL spectra is the microcavity effect, which greatly depends on the device structure.[10] However, the nearly same device structure can not make sense that it caused the total difference of EL spectra between TPA-PIM and TPA-PPI devices, except for the different emitter layers. Alternatively, the suppressed intramolecular vibration of the flexible TPA-PIM in solid state device may induce the narrowed EL spectra as in the frozen state of low temperature. Meanwhile, the inevitable vibration splitting in the strongly rigid phenanthro[9,10-*d*]imidazole structure of TPA-PPI may be enhanced in OLEDs to produce the large full peak width with red-shifted CIE coordinate. Thus we tentatively propose some possible explanations responsible for the large difference of CIE coordinate between TPA-PIM and TPA-PPI device. It could be attributed to the suppressed vibration splitting of the EL spectrum due to the full twisting molecular structure and the possible weak microcavity effect in TPA-PIM case as well.
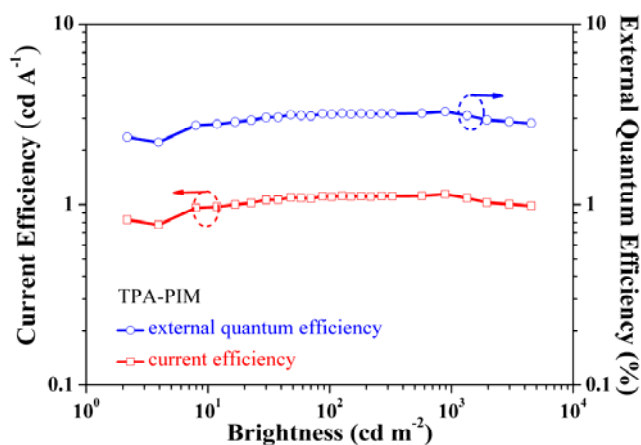

Figure 3. The current efficiency-brightness-external quantum efficiency curve of multilayered OLED based on TPA-PIM as emitter with device structures of ITO/PEDOT:PSS/NPB/TCTA/TPA-PIM/TPBi/ LiF/Al.

The EL device of TPA-PIM also exhibited an excellent efficiency performance, with a maximum luminous efficiency of 1.14 cd A^{-1}, a maximum power efficiency of 0.79 lm W^{-1}, a maximum brightness of 4510 cd m^{-2}, and a maximum external quantum efficiency (η_{ext}) of 3.28 % (Figure 3). Considering the saturated deep-blue emission with CIE coordinate of (0.161, 0.046), these values are among the best results ever reported[8,11]. Assuming the light out-coupling efficiency of 20 % and the 100 % hole-electron recombination in OLED, we estimated the exciton utilization efficiency of nearly 27 % on the basis of quantum efficiency in TPA-PIM device, which was similar to that in TPA-PPI device and broke through the spin statistics limit of 25% (singlet/triplet ratio ~ 1/3). This breakthrough was ascribed to the possible RISC process in the high-lying CT state as we suggested.[9] Moreover, the TPA-PIM device also exhibited an excellent efficiency stability with nearly none roll-off on the current efficiency and external quantum efficiency with an increasing brightness or current density during the whole driving voltage. Based on luminances of 100 cd m^{-2} (or 1000 cd m^{-2}), the TPA-PIM

device still showed a high current efficiency of 1.10 cd A^{-1} (or 1.08 cd A^{-1}) and an external quantum efficiency of 3.16% (or 3.11%). Meantime, EL spectra of TPA-PIM device also exhibited a good color stability with nearly the same CIE coordinates in the whole voltage range (Figure S8).

In summary, a fully twisting donor-acceptor molecule TPA-PIM was obtained with a maximum quantum efficiency of 3%, a CIE coordinate of (0.161, 0.046), and an extraordinary narrow FHWM of 35 nm in EL spectra from its multilayered non-doped device. The excellent color saturation in TPA-PIM could be ascribed to its fully twisting molecular structure due to the suppressed vibration splitting leading to the narrowed EL spectra in solid state or the possible weak microcavity effect in TPA-PIM device. Overall, the fully twisting structural TPA-PIM may serve as an excellent color saturation deep-blue emitter in OLEDs.

Notes and references

*a*State Key Laboratory of Supramolecular Structure and Materials,Jilin University, Changchun, 130012, P. R. China. Fax: +86 431 85168480; Tel: +86 431 85168480; E-mail: yangbing@jlu.edu.cn.
*b*College of Chemistry, Jilin University, Changchun, 130012, P.R. China.
*c*Institute of Polymer Optoelectronic Materials and Devices, State Key La boratory of Luminescent Materials and Devices, South China University of Technology, Guangzhou 510640, P. R. China.

† Electronic Supplementary Information (ESI) available: [details of synthesis, instruments, and charactions including photophysical, thermal, electrochemistry, and so on]. See DOI: 10.1039/b000000x/

1   C. W. Tang and S. A. VanSlyke, *Appl. Phys. Lett.*, 1987, **51**, 913; Y. G. Ma, H. Zhang, J. C. Shen, C. Che, *Synth. Met.*, 1998, **94**, 245.
2   M. Zhang, S. F. Xue, W. Y. Dong, Q. Wang, T. Fei, C. Gu and Y. G. Ma, *Chem. Commun.*, 2010, **46**, 3923.
3   B. Wei, J. Z. Liu, Y. Zhang, J. H. Zhang, H. N. Peng, H. L. Fan, Y. B. He, and X. C. Gao, *Adv. Funct. Mater.*, 2010, **20**, 2448.
4   J. W. G. Hunt, Measuring Color, Ellis Horwood, Chichester, 1980; Z. Q. Jiang, Z. Y. Liu, C. L. Yang, C. Zhong, J. G. Qin, G. Yu, Y. Q. Liu, *Adv. Funct. Mater.*, 2009, **19**, 3987.
5   Z. Q. Gao, Z. H. Li, P. F. Xia, M. S. Wong, K. W. Cheah, and C. H. Chen, *Adv. Funct. Mater.*, 2007, **17**, 3194; Z. Q. Jiang, Z. Y. Liu, C. L. Yang, C. Zhong, J. G. Qin, G. Yu, and Y. Q. Liu, *Adv. Funct. Mater.*, 2009, **19**, 3987.
6   Y. H. Kim, H. C. Jeong, S. H. KIM, K. Yang, and S. K. Kwon, *Adv. Funct. Mater.*, 2005, **15**, 1799.
7   Z. M. Wang, P. Lu, S. M. Chen, Z. Gao, F. Z. Shen, W. S. Zhang, Y. X. Xu, H. S. Kwok and Y. G. Ma, *J. Mater. Chem.*, 2011, **21**, 5451; H. H. Chou, Y. H. Chen, H. P. Hsu, W. H. Chang, Y. H. Chen, and C. H. Cheng, *Adv. Mater.*, 2012, **24**, 5867.
8   Z. Gao, G. Cheng, F. Z. Shen, S. T. Zhang, Y. N. Zhang, P. Lu, Y. G. Ma, *Laser & Photon. Rev.*, 2014, **8**, L6; Z. Gao, Y. L. Liu, Z. M. Wang, F. Z. Shen, H. Liu, G. N. Sun, L. Yao, Y. Lv, P. Lu, and Y. G. Ma, *Chem. Eur. J.*, 2013, **19**, 2602.
9   W. J. Li, D. D. Liu, F. Z. Shen, D. G. Ma, Z. M. Wang, T. Feng, Y. X. Xu, B. Yang, and Y. G. Ma, *Adv. Funct. Mater.*, 2012, **22**, 2797; W. J. Li, Y. Y. Pan, R. Xiao, Q. M. Peng, S. T. Zhang, D. G. Ma, F. Li, F. Z. Shen, Y. H. Wang, B. Yang, Y. G. Ma, *Adv. Funct. Mater.*, 2013, DOI: 10.1002/adfm.201301750.
10 S. Tokito, T. Tsutsui, and Y. Taga, *J. Appl. Phys.*, 1999, **86**, 2407; S. H. Cho, J. R. Oh, H. K. Park, H. K. Kim, Y. H. Lee, J. G. Lee, and Y. R. Do, *Opt. Express*, 2010, **18**, 1099.

11 C. C. Wu, Y. T. Lin, K. T. Wong, R. T. Chen, Y. Y. Chien, *Adv. Mater.*, 2004, **16**, 61; D. H. Yu, F. C. Zhao, Z. Zhang, C. M. Han, H. Xu, J. Li, D. G. Ma, P. F. Yan, *Chem. Commun.*, 2012, **48**, 6157.